Experiments with Light and Heavy Nuclei at HERMES

G. van der Steenhoven

Nationaal Instituut voor Kernfysica en Hoge-Energiefysica (NIKHEF),
P.O. Box 41882, NL-1009 DB Amsterdam, The Netherlands

Abstract: The physics prospects for using light and heavy nuclear targets in fixed-target experiments at HERMES are discussed. The kinematics of such experiments imply that the measurements can be used as a sensitive probe of the space-time dynamics of deep-inelastic scattering (DIS), enabling investigations of quark propagation and colour transparency. Moreover, the dilute internal gas targets used at HERMES make it possible to detect low-energy recoil products, that can be used to tag certain classes of DIS events. In this way neutron structure function data can be measured that do not suffer from ambiguities related to the structure of the deuteron. Moreover, new information on the origin of the EMC effect and the breaking of the Gottfried Sum Rule can be obtained.

1 Introduction

The HERMES experiment makes use of the HERA polarized electron (or positron) beam, which is interacting with a (fixed) polarized internal gas target flowing through a thin-walled storage cell. The deep-inelastic scattering events are observed with the HERMES (forward-angle) spectrometer, which also enables a fairly good identification of the hadronic final state. HERMES has started to produce first data on the neutron spin-structure function in 1995.

By injecting (polarized) nuclear targets into the storage cell, the HERMES set-up can be used for two new classes of experiments: (i) measurements in which the nucleus acts as a 'femtometer' detector; and (ii) measurements in which the deep-inelastic structure functions are tagged by detecting an additional hadron in the final state. The first class of experiments enables the study of quark propagation in the medium and the possible observation of colour transparency. The second type of experiments makes it possible to measure neutron structure functions without uncertainties related to nuclear corrections. Moreover, information can be obtained on the origin of the EMC effect, and the break down of the Gottfried Sum Rule. These experiments are discussed in more detail in sections 2 and 3, respectively.

The conditions for electro-nuclear fixed target experiments at HERMES are unique. The kinematics are well-matched to the length scales involved in hadron formation (see section 1.1), and the use of internal gas targets makes it possible to detect low-energy recoil products, which is impossible at other deep-inelastic scattering facilities (see section 1.2). Together these conditions are well fit for measurements that address the unknown transition from the region where perturbative QCD applies (at high Q^2) to the non-perturbative domain at lower-Q^2 values.

In this report the prospects for using nuclear targets at HERMES are summarized. The discussions are brief when dedicated contributions exist that provide all necessary detail (section 2). In other cases the summaries are longer, in particular when the specific contributions do not include any count-rate estimates (section 3). Some practical considerations concerning the realisation of such experiments at HERMES are presented in the last section of this report.

1.1 Kinematics

Three length scales enter the description of the semi-inclusive processes in deep-inelastic scattering that are at the basis of most of the physics issues addressed in this report:

- The coherence length describes the hadronic $q\bar{q}$ fluctuation of a virtual photon

$$l_C \approx \frac{2\hbar c\nu}{Q^2 + m^2_{q\bar{q}}} = \frac{\hbar c}{m_p x(1 + \frac{m^2_{q\bar{q}}}{Q^2})} \approx \frac{\hbar c}{m_p x}, \tag{1}$$

  where ν represents the energy transfer, Q^2 the four-momentum transfer, $m_{q\bar{q}}$ the mass of the hadronic fluctuation and x is the usual Bjorken-scaling parameter ($\frac{Q^2}{2m_p\nu}$). Note that the last equality sign only holds in the high-Q^2 limit. A typical value of l_C for HERMES kinematics is 3 fm, whereas l_C is much larger (10 - 30 fm) for the deep-inelastic lepton scattering experiments at CERN (NMC) and Fermilab (E665).

- The formation length describes the distance between the initial lepton interaction vertex and the hadron formation point:

$$l_F \approx \frac{2\hbar c\nu}{\delta m^2_V}, \tag{2}$$

  with δm^2_V the characteristic squared-mass difference between low-lying vector-meson states ($\delta m^2_V \sim 1$ GeV^2). A typical value of l_F for HERMES kinematics is 5 fm, whereas l_F is much larger (50 fm) at NMC and E665.

- The transverse size of the hadronic fluctuation is mainly relevant for colour-transparency studies:

$$r_\perp \approx \frac{5\hbar c}{Q}. \tag{3}$$

  Depending on the Q^2-range selected the values for $r_\perp$ range from about 0.3 fm to 0.7 fm, but usually considerably smaller than the radius of a nucleon.

It is seen that the sizes of l_F and l_C are commensurate with nuclear dimensions for deep-inelastic scattering at HERMES energies. Hence, experiments that want to exploit the nuclear medium, and thus want to maximize its influence, are best carried out at HERMES (as compared to E665, SMC, NMC, etc.)

1.2 Internal nuclear targets at HERMES

The advantages of using an internal target in semi-inclusive deep inelastic scattering are twofold: (i) a high level of undiluted target polarization can be obtained; and (ii) the use of a dilute gas allows the detection of low-energy recoil products.

In order to study the feasibility of electro-nuclear experiments at HERMES, the type of nuclei that can be used and the maximum luminosity that can be obtained must be determined.

The HERMES set-up has already been operated with polarized and unpolarized ^{1}H, ^{2}H, and ^{3}He targets. For heavier targets the exact species is not important as the experiments discussed only require a certain (varying) amount of nuclear matter. Hence, the only requirement is that a fairly large A-range is covered.

To avoid heating the target, considerations are restricted to the gaseous elements ^{4}He, N, O, F, Ne, Cl, Ar, Kr, Xe, and Rn. These have boiling points at atmospheric pressure of 4.2, 77, 90, 85, 27, 239, 87, 121, 166, and 211 K, respectively. The elements F and Cl have to be excluded, as they are highly reactive with steel and human lung tissue. Moreover, the elements oxygen (O) and radon (Rn) are not considered either. Compared to oxygen the nearby element nitrogen (N) is much easier to handle, while Rn is radioactive and difficult to provide.

It is worth noting that the DESY machine group will resist efforts to use a ^{4}He target because they use ^{4}He for leak checking and any ^{4}He contamination will reduce their sensitivity. The remaining elements (^{3}He, ^{14}N, ^{20}Ne, ^{40}Ar, ^{84}Kr, and ^{131}Xe) cover a large enough A-range, and their use is not expected to be opposed by the DESY machine group, provided that the beam life time is not affected.

Atomic bremsstrahlung of beam positrons in the HERMES target reduces the beam lifetime. In the absence of other beam-loss mechanisms, the lifetime would be:

$$T_{\rm targ} \approx T_0 \left[Z(Z+1) \left(\ln \frac{183}{Z^{1/3}} \right) \left(\frac{n}{8.1 \times 10^{25}\,\rm atoms/cm^2} \right) \right]^{-1}, \qquad (4)$$

where n is the target thickness and $T_0 = 21\,\mu$s is the revolution time of HERA [1]. In order to prevent a significant reduction in the ~ 10 h beam lifetime, HERMES is required to run with $T_{\rm targ} \geq 45$ h. Thus the maximum thickness for unpolarized targets is [4]:

$$n_{\rm max} = \frac{1.05 \times 10^{16}\,\rm atoms/cm^2}{Z(Z+1)\ln(183 Z^{-1/3})}. \qquad (5)$$

Figure 1 exhibits the corresponding luminosity L_A for a beam current of 35 mA (taken from ref. [4]). It is concluded that the *nucleon* luminosity is not decreasing steeply with A. Therefore, the luminosity that is available for nuclear targets at HERMES is not expected to be a strong limiting factor.

2 A femtometer detector in deep-inelastic scattering

The space-time evolution of hadron-formation in deep-inelastic scattering cannot be described from first principles in QCD. Hence, several models have been developed to describe this non-perturbative process. In order to calibrate and select among these models it is desirable to perform experiments in which hadron formation is actually modified by embedding it in a medium of varying density, i.e. using nuclear targets.

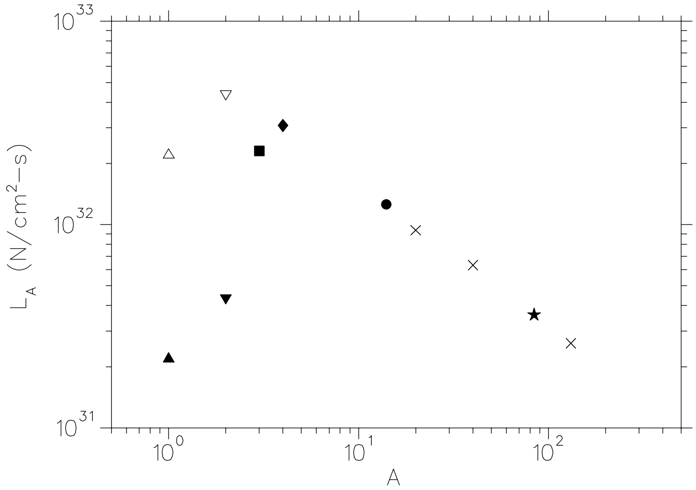

Figure 1: Maximum ($I_{\rm beam}$ = 35 mA) obtainable luminosity in nucleons/cm^2-s for ^{1}H, ^{2}H, ^{3}He, ^{4}He, N, Ne, Ar, Kr, and Xe [4]. For ^{1}H and ^{2}H the open symbols are the beam lifetime limits for unpolarized running and the closed circles are the ABS limits for polarized running.

2.1 Quark Propagation

By comparing the production of leading hadrons (such as pions, kaons, lambda's and protons) in deep-inelastic scattering off nuclei to the production off nucleons, one can determine the attenuation of those hadrons in the nuclear medium. In the kinematic domain accessed by HERMES these attentuation ratios R_A can be measured for various nuclei and hadrons in such a way that $l_F \sim R_{nucleus}$. Consequently, the results are expected to be extremely sensitive to the model assumed for the formation process of the hadron. In fact, such data can be used to determine the hadron formation time τ_{form}. Moreover, the good particle identification capabilities offered by the HERMES spectrometer (especially if it is also equiped with a ring-imaging cherenkov (RICH)), allows a separate determination of attenuation ratios for different hadrons. As the formation time models strongly depend on the hadron mass, the results for different hadrons provide additional constraints on such models.

Few measurements of R_A exist. At high ν some data have been reported by EMC [2], which are all very close to unity. In the low energy domain ($2 \leq \nu \leq 20$ GeV), a significant hadronic attenuation has been observed in a single poor-statistics measurement taken at SLAC [3] (with hardly any particle idenfication). Hence, HERMES can make a unique contribution to this field by performing precise measurements of R_A in the energy domain which is expected to be most sensitive to the hadron formation process, and by measuring the hadron formation time. Detailed count-rate estimates for such experiments are presented in ref. [4], while Kopeliovich et al. [5] and Pavel [6] discuss various models for hadronization processes in nuclei.

Further information on the hadron formation process can be obtained by searching for slow protons and/or neutrons ($\lesssim 2$ GeV) that are produced in semi-inclusive deep-inelastic scattering events. If these nucleons are normal hadronization products the yield should be proportional to A, but if they result from secondary interactions of leading hadrons the rate will increase faster. Hence, the measurement of slow protons and neutrons can be used to determine the number of secondary interactions in deep inelastic scattering [8].

To date only one result has been reported on the observation of slow neutrons in deep inelastic scattering. At Fermilab [7] a surprisingly low number of slow neutrons was observed, suggesting that only few reinteractions occur at high energy. At HERMES we expect a larger number of neutrons per DIS-event, because of the increased influence of the nuclear medium on the quark propagation process. A simple count rate estimate shows that one can expect about 1000 slow neutron events in 3 months of running time using a Xenon target at a luminosity of $3\ 10^{31}$ N/cm^2/s and a 100 msr time-of-flight scintillator array.

2.2 Colour Transparency

Colour transparancy (CT) represents one of the few QCD-based predictions that have not been verified experimentally (the other well-known one being the quark-gluon plasma). In the case of CT it is predicted that a hadron propagating through a medium will experience hardly any (final-state) interactions if the hadrons are produced in configurations with small transverse size $r_\perp$ and have a long enough expansion time. The kinematics at HERMES imply that $r_\perp \sim 0.3$ fm, while the coherence length is still small such that the interactions occur inside the nuclear medium. Moreover, the (missing) energy resolution ($\lesssim 0.5$ GeV) offered by the HERMES spectrometer enables the observation of (almost) exclusive reaction channels, which makes the interpretation of the data considerably less ambiguous. These unique properties of the HERMES set-up are exploited in several proposals for CT-measurements that are summarized in this section.

Traditionally, exclusive (high z) production of protons has been used for CT studies. However, Hüfner and Kopeliovich [9] have argued that it may be very difficuly to obtain unambiguous evidence for CT from such measurements. Instead they advocate the use of ρ^0 or ϕ production. It turns out that exclusive coherent or incoherent (low-t) production of vector mesons is highly sensitive to the occurrence of CT. In ref. [4] it is shown that a modest 30 fills per target could already provide significant data on colour transparency in the exclusive ρ^0 channel. Moreover, these data can be used to determine the time it takes for an initial point-like configuration to expand to its full physical size (expansion time).

Apart from the aforementioned unpolarized measurements, Frankfurt et al. [10] have argued in favour of using a tensor polarized deuterium target for CT studies. They have demonstrated large effects on the tensor analyzing power in proton production on deuterium. This effect can be attributed to the fact that at high t the relative importance of CT is larger for the d-state as compared to the s-state in deuterium.

Finally, it would be desirable to isolate the coherent ρ^0 production channel, which is theoretically easier to approach. Experimentally, one could isolate the (exclusive) coherent channel from the dominant incoherent channel by detecting a recoiling light target nucleus [11], which can only be achieved with an internal target such as is available at HERMES.

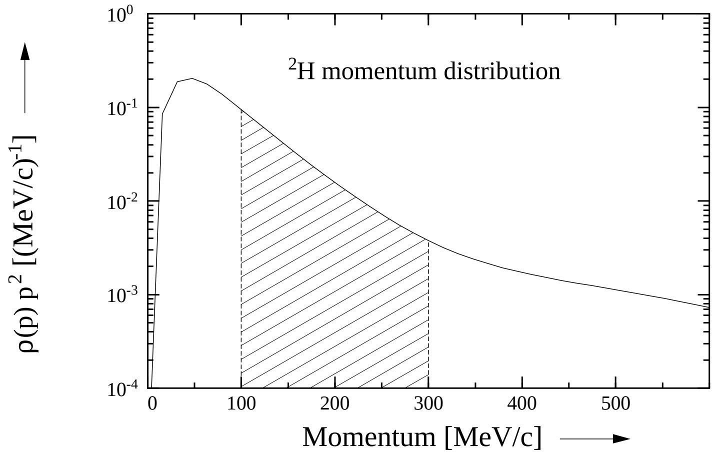

Figure 2: Deuteron wave function, $\rho(p)p^2 = |\psi(p)|^2 p^2$, as a function of the nucleon momentum. The hatched area indicates the relevant momentum range for a neutron tagging experiment.

3 Tagged Structure Functions

3.1 Neutron Structure Functions

The (spin) structure functions of the neutron are usually measured by subtracting ^{2}D and ^{1}H data. The evaluation of the neutron structure functions from such a subtracted data requires the application of nuclear corrections that account for the dynamics of the neutron inside the deuteron. These corrections are reasonably well under control for unpolarized structure functions provided that $x \lesssim 0.5$, but are less well known for the *spin* structure functions. Hence, there is interest in an unambiguous determination of the unpolarized structure function $F_2^n(x)$ for $x \to 1$ and $g_1^n(x)$ in the entire $x-$domain.

Alternatively, the neutron structure functions can be measured in deep inelastic scattering (DIS) off a deuteron target with simultaneous detection of a recoiling proton, i.e the proton acts as a spectator which tags a DIS-events off a neutron [16]. The method assumes the dominance of the spectator mechanism. Simula [17] has investigated the relative merits of various scaling variables that can be used to identify the spectator mechanism for deep-inelastic electron scattering off a deuteron target.

The cross section for the observation of a spectator proton in deep-inelastic scattering off a deuteron target reads:

$$\sigma_{\text{recoil}} \sim F_2^n(\frac{x}{2-\alpha})|\psi(\alpha, p_\perp)|^2, \tag{6}$$

where the neutron structure function F_2^n is evaluated at a rescaled momentum fraction with α the lightcone momentum fraction carried by the spectator:

$$\alpha = \frac{\sqrt{m_p^2 + p^2} - \vec{p} \cdot \hat{q}}{m_p} \tag{7}$$

The second term in the cross-section expression, $\psi(\alpha, p_\perp)$, essentially represents the nucleon wave function of the deuteron, which is illustrated in figure 2.

The yield of a neutron-tagging experiment is determined by the lower and upper limits of the integral $\int |\psi(p)|^2 p^2 dp$. The lower limit is set by the detection threshold of the low-momentum recoil detectors that will be placed close to the storage cells in the HERMES vacuum chamber. The exact value of the lower limit will depend on the wall thickness of the storage cell. In a 100 μm aluminum wall, as is presently used at HERMES, a proton (passing under 45 degrees) of 4.2 MeV, i.e. 88 MeV/c momentum, will be stopped. Hence, it is not unrealistic to use a lower limit of 100 MeV/c. The upper limit is determined by the uncertainty in the knowledge of the deuteron wave function, for which usually 300 MeV/c is taken, i.e. the domain where the d-state starts to dominate.

Under the assumption that recoil detection equipment covers 400 msr of the non-forward acceptance of the HERMES storage cell, the count-rate of a neutron tagging experiment has been estimated. The proton kinetic-energy acceptance is assumed to range from 2 to 30 MeV. A target thickness of $1 \cdot 10^{14}$ atoms/cm^2 has been taken, and an average positron current of 30 mA. With a typical target polarization of 80% and a beam polarization of 50%, we arrive at the error bars for F_2^n and the asymmetry A_1^n listed in table 1. The uncertainties shown correspond to 400 hours (or 50 fills) of data taking for each spin direction.

$x-$bin	$< Q^2 >$	δF_2^n	$\delta A_1^n\rfloor_{tag}$	$\delta A_1^n\rfloor_{D-H}$
0.02 - 0.03	1.2	1.9 %	0.055	0.018
0.04 - 0.06	1.9	1.3 %	0.046	0.016
0.10 - 0.15	3.3	1.1 %	0.059	0.026
0.20 - 0.30	4.3	1.2 %	0.092	0.051
0.40 - 0.50	5.5	2.2 %	0.253	0.167
0.60 - 0.70	9.1	7.5 %	0.772	0.520

Table 1: *Estimated statistical uncertainties in F_2^n and A_1^n for some selected $x-$bins in a neutron-tagging experiment off a polarized ^2H target. The statistical uncertainties associated with the traditional ^2D - ^1H subtraction method (also for 800 hours of beam time) are displayed in the last column.*

From table 1 it is seen that the recoil method leads to small error bars for F_2^n, which is of particular interest at high values of x. A measurement in this domain is of particular interest in view of the existing predictions for the ratio F_2^n/F_2^p, which in the limit of $x \to 1$ should approach the value 3/7 according to pQCD, while models based on the dominance of a scalar valence di-quark component in the nucleon predict this ratio to approach the value 1/4 [18]. Because of the relatively large nuclear corrections at large values of x, the existing data cannot distinguish between these conflicting predictions. The recoil method will enable a precise measurement of F_2^n/F_2^p at high x, as it does not suffer from such uncertainties [19].

The statistical errors anticipated for $A_1^n\rfloor_{tag}$ are significantly larger than those obtained in the $D - H$-subtraction method (taken from [12]). This is to be expected from the fact that the recoil proton cannot be detected over its full 4π phase space. However, the systematic uncertainty is expected to be considerably less. This can best be seen from ref. [13], where it is shown that the difference between the asymmetry for a free neutron and one bound in deuterium can be as large as a factor of 2 (depending on x). Moreover, if a laser-driven source comes available for HERMES the (polarized) target thickness can be improved by a factor of 4, yielding error bars for A_1^n that are similar to the ones quoted in [12] for the (^{2}D - ^{1}H) subtraction method.

It is concluded that neutron tagging, which is virtually absent of nuclear-physics complications, can provide important neutron structure function data in the nearby future.

3.2 The origin of the EMC Effect

The neutron-tagging technique can be extended to study the possible origin of the EMC effect, i.e. the unexplained observation of an A-dependence of the unpolarized structure function $F_2(x)$. The concept is based on the known importance of nucleon-nucleon correlations in nuclei. As a consequence the momentum of a recoiling backward-going proton in deep-inelastic scattering is a direct measure of the momentum of the struck neutron. The dominance of this mechanism for backward-going protons has been demonstrated in ref. [14] for deep-inelastic neutrino scattering off ^{2}H (also see ref. [16]). Using the neutron-tagging technique it is thus possible to measure the dependence of $F_2^n(x)$ on the momentum of the parent neutron in which the struck quark resided.

The nucleon-momentum dependence of $F_2(x)$ can be instrumental in discriminating among models that have been developed to explain the EMC effect in the $x-$range between 0.1 and 0.8. While models assuming an intrinsic modification of $F_2(x)$ in general predict a strong increase of the EMC-effect with nucleon momentum (or effectively the nucleon density), models based on nuclear dynamics do not predict such effects.

There are essentially two proposals for studying the origin of the EMC effect in this way. Melnitchouk, Sargsian and Strikman [19] have suggested to use a ^{2}H target. As the high-momentum tail of the nucleon wave function is expected to be roughly the same for all nuclei, it is advantageous to use a ^{2}H target for which the wave function is well known (see figure 2). Alternatively, the tagged structure functions are measured on various target nuclei, which enables the variation of the nuclear density involved. However, a word of caution is appropriate in the latter case as part of the slow protons may be due to hadronization or rescattering of fragmentation products [20]. Simula has considered some of these complications in his contribution to the workshop [21].

In order to assess the feasibility of such tagged-structure function measurements, we have evaluated the error bars to be expected for 800 hours of data taking, i.e. about 100 fills, at a luminosity of $1.25 \cdot 10^{32}$ nucleons/cm^2/s on a ^{14}N unpolarized gas target. Assuming the availability of 800 msr of recoil-detection equipment one arrives at the results displayed in figure 3 for the ratio of the semi-inclusive over the inclusive deep-inelastic cross section [23].

It is seen that precise data can be obtained in about half a year worth of data taking. Measurements of this type do not exists nor are foreseen at any other laboratory.

3.3 The break-down of the Gottfried Sum Rule

In the quark-parton model one can relate the difference between the structure functions of the proton and the neutron to the difference between the u and d sea-quark distributions:

$$S_G = \int \frac{1}{x}(F_2^p(x) - F_2^n(x))dx = \frac{1}{3} - \frac{2}{3}\int (\bar{d}(x) - \bar{u}(x))dx. \tag{8}$$

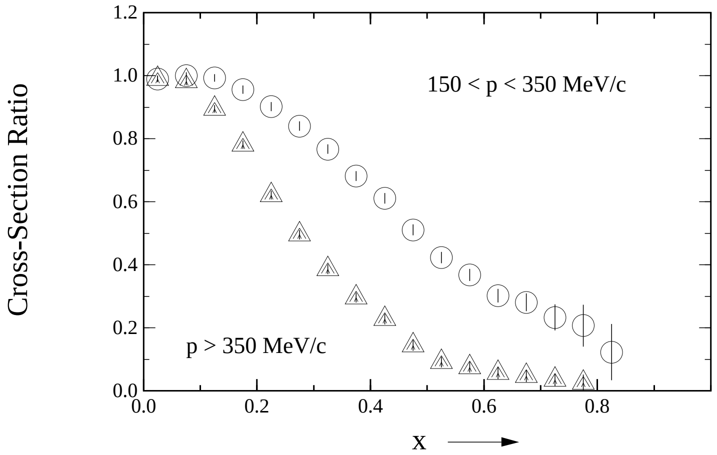

Figure 3: Ratio of cross sections for semi-inclusive and inclusive deep inelastic scattering off a ^{14}N target. The solid circles represent the data tagged by a proton of a momentum between 150 and 350 MeV/c, while the triangles correspond to events with proton momenta larger than 350 MeV/c [23].

Under the assumption that the sea is u-d flavour symmetric, the Gottfried Sum Rule is obtained [24], i.e., $S_G = \frac{1}{3}$. It came as a surprise when NMC and SLAC [25] found that $S_G = 0.240 \pm 0.016$, implying that the sea is flavour asymmetric, i.e. $\bar{d}(x) \neq \bar{u}(x)$.

Meson-cloud models [26] turned out to be able to reproduce the low value of S_G, i.e. $S_G\rfloor_{meson-cloud} \approx 0.1 - 0.2$. This result gives rise to the question whether or not the nucleon has an explicit mesonic component. In order to study the validity of these meson-cloud models, several experiments have been proposed that could be carried out at HERMES.

In deep inelastic scattering (DIS) off a ^{3}He target, for instance, the observation of recoiling ^{3}H nuclei identifies a possible DIS-event off a positive pion. As opposed to the nucleon case there can hardly be any contamination from target fragmentation as the fragmentation function of a quark leading to a ^{3}H nucleus must be vanishingly small, i.e. $D_{qq}^{^3H}(z) = 0$. The kinematics and cross section for such an experiment are discussed by Dieperink [22].

It has also been proposed to measure the polarization of a semi- inclusively produced Δ^{++} or a Λ from the angular distribution of the decay products. In simple models of di-quark fragmentation processes this polarization is very close to zero, while meson cloud models predict a very strong polarization signal [27].

For either of these measurements extensions and changes have to be made to the HERMES set-up, including – once again – the option to detect low-mass recoil products outside the acceptance of the forward spectrometer.

4 Outlook

A considerable number of different measurements have been proposed that could make use of light or heavy nuclear targets at HERMES. More details are given in the contributions to the Workshop, which are also included in the proceedings. For many of the proposed measurements count-rate estimates exist, that show the feasibility of most of the proposed experiments.

In order to fully exploit the ideas discussed in this report (with the various contributions attached to this report), several additions to the HERMES set-up need to be considered:

- Gaseous targets ^{3}He, ^{14}N, ^{20}Ne, ^{40}Ar, and ^{131}Xe need to be available and be allowed to use.
- A ring-imaging cherenkov counter should replace the existing threshold Cherenkov counter in order to improve the particle identification of the hadronic final state in HERMES. A RICH will be of particular interest for studies of quark propagation in nuclei. (Alternatively, a second threshold cherenkov counter could be used.)
- Large solid-angle recoil detection equipment is needed. As protons with extremely low proton momenta need to be detected, it would be natural to consider detectors that will be mounted inside the scattering chamber. A large neutron time-of-flight wall could be of similar interest in order to tag the proton structure functions.
- For some of the measurements -especially those of the neutron spin structure function through recoil tagging- a high-intensity polarized deuterium target needs to available, i.e. a laser-driven source or an upgraded ABS system .

A full-scale programme investigating the non-perturbative domain of QCD by exploiting light and heavy nuclear targets at HERMES, could start as early as 1999. Test experiments can be prepared during the on-going programme of spin-structure functions measurements.

References

[1] M. Düren, *Effect of the Electron Beam Tails at the HERMES Collimators*, DESY-HERMES 90-01 (1990).

[2] M. Arneodo, Phys. Rep. 240 (1994) 301.

[3] L.S. Osborne *et al.*, Phys. Rev. Lett. 40 (1978) 1624.

[4] T.G. O'Neill and G. van der Steenhoven, *Proposal for Unpolarized $A > 3$ Running at HERMES*, DESY-HERMES 96-16 (1996); and contribution to this workshop (working group 8) on *Color Transparency and Quark Propagation*

[5] B. Kopeliovich, J. Nemchik and E. Predazzi, contribution to this workshop (working group 8) on *Hadronization in Nuclear Environment.*

[6] N. Pavel, contribution to this workshop (working group 8) on *Study of Hadronization in Deep-Inelastic Lepton-Nucleus Scattering at HERMES*

[7] M.R. Adams *et al.*, Phys. Rev. Lett. 74 (1995) 5198.

[8] M. Strikman, M.G. Tverskoy, M. Zhalov, contribution to this workshop (working group 8) on *Soft Neutron Production - a window to the Final State Interaction in Deep-Inelastic Scattering*

[9] J. Hüfner andd B. Kopeliovich, contribution to this workshop (working group 8) on *Towards Study of Color Transparency with Medium Energy Electron Beams.*

[10] L. Frankfurt, M. Sargsian, M. Strikman, contribution to this workshop (working group 8) on *Near Threshold Large Q^2 Electroproduction off Polarized Deuterium.*

[11] L. Frankfurt, W. Koepf, J. Mutzbauer, G. Piller, M. Sargsyan, M. Strikman, contribution to this workshop (working group 8) on *Coherent ρ^0 production from polarized deuterium.*

[12] The HERMES collaboration, *HERMES Technical Design Report*, July 1993.

[13] R.M. Woloshyn, Nucl. Phys. **A496** (1989) 749.

[14] G.D. Bosveld, A.E.L. Dieperink, O. Scholten, Phys. Rev. **C 45** (1992) 2616.

[15] G.D. Bosveld, A.E.L. Dieperink, A.G. Tenner, Phys. Rev. **C 49** (1994) 2379.

[16] L.L. Frankfurt and M. Strikman, Phys. Rep. **76** (1981) 215.

[17] S. Simula, *Semi-Inclusive Deep Inelastic Scattering off the Deuteron and the Neutron to Proton Structure Function Ratio*, INFN-ISS 96/2, and contribution to this workshop (working group 8) on *Investigation of the neutron structure function via semi-inclusive deep inelastic scattering off the deuteron.*

[18] W. Melnitchouk and A.W. Thomas, Phys. Lett. **B 377** (1996) 11.

[19] W. Melnitchouk, M. Sargsian, M. Strikman, contribution to this workshop (working group 8) on *Tagged-Structure Functions of the Deuteron and the origin of the EMC effect*

[20] J. Guy et al, Phys. Lett. **B 229** (1989) 421.

[21] S. Simula, contribution to this workshop (working group 8) on *Semi-Inclusive Deep Inelastic Scattering off Nitrogen.*

[22] A.E.L. Dieperink, contribution to this workshop (working group 8) on *Pobing the nucleon meson-cloud in semi-inclusive deep inelastic scattering: tagging of ^3He*

[23] R.S. Hicks and G. van der Steenhoven, *The measurement of nuclear decay products in deep inelastic reactions*, NIKHEF-HERMES internal note (1991).

[24] K. Gottfried, Phys. Rev. Lett. **18** (1967) 1174.

[25] P. Amaudruz at al., Phys. Rev. Lett. **66** (1991) 2712; A. Baldit et al., Phys. Lett. **B 332** (1994) 244.

[26] A.W. Thomas, Phys. Lett. **126 B** (1983) 97.

[27] W. Melnitchouk and A.W. Thomas, contribution to this workshop (working group 8) on *Meson Cloud Signatures in Semi-Inclusive Deep-Inelastic Scattering from Polarized Nucleons.*